Re: CAN-08-3620R

Integral Role of Transcription Factor 8 in the Negative Regulation of Tumor Angiogenesis

Takayuki Inuzuka,[1] Masumi Tsuda,[1] Shinya Tanaka,[2] Hideaki Kawaguchi,[1] Yujiro Higashi,[3] and Yusuke Ohba[1]

[1]Laboratory of Pathophysiology and Signal Transduction, and [2]Laboratory of Molecular and Cellular Pathology, Hokkaido University Graduate School of Medicine, Sapporo, Japan, and [3]Department of Perinatology, Institute for Developmental Research, Aichi Human Service Center, Kasugai, Japan.

Running title: TCF8 negatively regulates angiogenesis

Keywords: angiogenesis; tumor angiogenesis; TCF8

Foot notes

Grant support: Grants-in-Aid for Scientific Research from the Ministry of Education, Culture, Sports, Science and Technology, Japan, and Japan Society for the Promotion of Science (JSPS), the Uehara Memorial Foundation, and the Mochida Memorial Foundation for Medical and Pharmaceutical Research. T.I. is a JSPS fellow.

Requests for reprints: Yusuke Ohba, Laboratory of Pathophysiology and Signal Transduction, Hokkaido University Graduate School of Medicine, N15W7, Kita-ku, Sapporo 060-8638, Japan. Phone: +81-11-706-5158; Fax: +81-11-706-7877; E-mail: yohba@med.hokudai.ac.jp

Note: Supplementary data for this article are available at Cancer Research Online

[4] Unpublished data

Abstract

Angiogenesis is involved in various physiological and pathological conditions, including tumor growth, and is tightly regulated by the orchestration of pro- and anti-angiogenic factors. Inhibition of vascular endothelial growth factor (VEGF), the best-established anti-angiogenic treatment in cancer, has demonstrated some effectiveness; however, the identification of novel regulators, whose function is independent of VEGF, is required to achieve better outcomes. Here, we show that transcription factor 8 (TCF8) is up-regulated in endothelial cells during angiogenesis, acting as a negative regulator. Furthermore, TCF8 is specifically expressed in the endothelium of tumor vessels. *Tcf8*-heterozygous knockout mice are more permissive than wild-type mice to the formation of tumor blood vessels in subcutaneously implanted melanoma, which appears to contribute to the more aggressive growth and the lung metastases of the tumor in mutant mice. Suppression of TCF8 facilitates angiogenesis in both *in vitro* and *ex vivo* models, and displays comprehensive cellular phenotypes, including enhanced cell invasion, impaired cell adhesion, and increased cell monolayer permeability due to, at least partly, MMP1 overexpression, attenuation of focal adhesion formation, and insufficient VE-cadherin recruitment, respectively. Taken together, our findings define a novel, integral role for TCF8 in the regulation of pathological angiogenesis, and propose TCF8 as a target for therapeutic intervention in cancer.

Introduction

Angiogenesis, the development of new blood vessels from existing ones, apart from being central to a variety of physiological phenomena, including tissue growth and repair, fetal development, and the female reproductive cycle, is crucial for supplying oxygen and nutrients to specific pathological tissues such as neoplasms (1, 2). The process of angiogenesis consists of multiple, interrelated steps, which are tightly regulated by the balance between pro- and anti-angiogenic factors (3, 4). First, angiogenic growth factors secreted from tissues in need of oxygen activate receptors present on endothelial cells in pre-existing vessels, which trigger subsequent angiogenic signaling. The activated endothelial cells release proteases such as matrix metalloproteases (MMPs), that degrade the basement membrane and extracellular matrices (ECMs) in order to escape from the pre-existing vessel walls and invade into surrounding tissues. The endothelial cells then proliferate into the surrounding matrix and form solid sprouts connecting neighboring vessels. As sprouts extend toward the source of the angiogenic stimulus, endothelial cells migrate in tandem, using adhesion molecule integrins. Finally, the endothelial cells stop proliferating and invading, strengthen cell-cell adhesion, and recruit other classes of supporting cells such as pericytes and smooth muscle cells to form a full-fledged vessel lumen. At this stage, the expression of genes classified as negative regulators with roles in vascular stabilization and differentiation is also induced; the absence of these factors results in excess vasculature with high remodeling activity, which leads to the formation of unsettled and aberrant blood vessels (5).

Among a range of angiogenic factors, vascular endothelial growth factor (VEGF) has been identified as the most potent and predominant (6), and thus VEGF inhibitors are utilized in cancer therapy to suppress tumor angiogenesis. Although these therapies yield certain outcomes, inhibition of VEGF alone might be insufficient to permanently halt angiogenesis. In fact, emerging evidence indicates that inhibition of single targets leads to the upregulation of additional angiogenic factors (7). Therefore, identification of other molecular targets with

distinct complementary mechanisms of action from that of VEGF is desired in order to construct an integrated treatment with anti-angiogenic agents, which yields a greater efficacy.

The two-handed zinc finger (ZF) homeodomain transcription factor TCF8, alternatively designated as δEF1, ZEB-1, Nil2, and Zfhxp1, has been implicated in a range of biological phenomena, including cancer invasion, cellular senescence, viral infection, bone metabolism, and T-cell and neuronal development (8-11). Because of the conserved DNA-binding property of two ZF–domain clusters, TCF8 regulates the expression of various molecules at the transcriptional level. Specifically, TCF8 functions as a transcriptional repressor of epithelial markers, including E-cadherin, and promotes epithelial-mesenchymal transition as well as the invasion of cancerous cells. In the cardiovascular system, δEF1 (the murine orthologue of TCF8) has been shown to regulate Smad-dependent gene induction, which results in abnormal intimal thickening after balloon injury in *δEf1*-heterozygous knockout (KO) mice (12). The human *Tcf8* gene encoded on 10p11.2 is implicated in posterior polymorphous corneal dystrophy, a disease characterized by abnormal proliferation of corneal endothelial cells and accumulation of type IVα3 collagen (13). Although these results raise the possibility that TCF8 might function in vascular endothelial cells, there is limited literature available that addresses this issue.

Here, we identify TCF8 as a negative regulator of angiogenesis *in vitro*, *ex vivo*, and *in vivo*. Additionally, tumor angiogenesis is significantly up-regulated in *Tcf8*-heterozygous KO mice, which leads to the more aggressive growth and the distant metastases of subcutaneously injected melanoma. Since the expression of TCF8 is independent of VEGF and is restricted within tumor-related blood vessels, our finding defines a novel mechanism for the negative regulation of pathological angiogenesis.

Materials and Methods

Reagents and antibodies. The MMP inhibitor GM6001 was obtained from CHEMICON International (Temecula, CA). Antibodies against TCF8 (ZEB1), α-SMA, β-actin, HA, and CD31 were purchased from Santa Cruz Biotechnology (Santa Cruz, CA), DAKO (Copenhagen, Denmark), Santa Cruz Biotechnology, Roche (Indianapolis, IN), and Abcam (Cambridge, UK), respectively. An antibody against TCF8 (AREB6) for mouse tissue staining was kindly provided by Dr K. Kawakami (Jichi Medical University, Tochigi, Japan).

Expression plasmids. Human TCF8 cDNA was obtained by RT-PCR of total RNA from HUVECs and was cloned into pCR-BluntII-TOPO (Invitrogen, Carlsbad, CA). To generate HA-tagged TCF8 expression vectors, the cDNA was subcloned into the XhoI and NotI sites of the pCXN2-3xHA vectors (14).

Cell culture and transfection. HUVECs were maintained in complete endothelial basal medium (EBM-2) and transfected with siRNA targeting the human TCF8 mRNA [si TCF8, (15)] using HiPerFect reagent (QIAGEN, Valencia, CA) according to the manufacturer's instructions. AllStars Negative Control siRNA (si Control, QIAGEN) was used as a control. The cells were analyzed after 48 or 72 h. Cells, which had been passaged 4 to 10 times, were used throughout the experiments. 293T cells were cultured in DMEM (Sigma, St. Louis, MO) supplemented with 10% FCS. Expression plasmids were introduced with FuGENE HD (Roche) according to the manufacturer's protocol

Tube formation assay. Tube formation by HUVECs on Matrigel (BD-Discovery Labware, Bedford, MA) was performed as described previously (16, 17) with some modifications. Each well of a 12-well plate was coated with 250 μl of 10 mg/ml Matrigel, and was filled with 7.5×10^4 cells in 1 ml of complete EGM-2. At the indicated times, ten images of the formed tubes were obtained for every well and the number of tubes was quantified, followed by total RNA extractions.

RNA isolation and RT-PCR. RNA isolation and RT-PCR were performed as described previously (18). Briefly, the total RNA was isolated from cells using an RNeasy Mini Kit (QIAGEN) according to the manufacturer's instructions. First strand cDNA was synthesized from 1.0 μg of total RNA by SuperScript III reverse transcriptase (Invitrogen). The primers used for PCR amplification were: GAPDH-F, 5'- GAAATCCCATCACCATCTTCCAGG-3'; GAPDH-R, 5'-CATGTGGGCCATGAGGTCCACCAC-3'; and TCF8-F, 5'-TGCACTGAGTGTGGAAAAGC-3'; TCF8-R, 5'-TGGTGATGCTGAAAGAGACG-3'. Real-time PCR was performed using a Light Cycler 480 and the Universal Probe Library system (Roche) for GAPDH and MMP1, and by using the SYBRGreen system for TCF8, respectively. Sequence for primers and probes used for real-time PCR were: GAPDH-F, 5'-AGCCACATCGCTCAGACAC-3'; GAPDH-R, 5'-GCCCAATACGACCAAATCC-3'; GAPDH-probe, 5'-TGGGGAAG-3'; and MMP1-F, 5'-GCTAACCTTTGATGCTATAACTACGA-3'; MMP1-R, 5'-TTTGTGCGCATGTAGAATCTG-3'; MMP1-probe, 5'-GGGAGAAG-3'. The same primers used in the conventional RT-PCR were used for TCF8. Data were normalized by the expression level of GAPDH in each sample.

Mice. *Tcf8* (*δEf1*) heterozygous KO mice were described previously (10), and were backcrossed onto C57BL/6. Wild-type (C57BL/6) mice were purchased from CLEA Japan (Tokyo, Japan). Mice were maintained under specific pathogen-free conditions, and mice breeding and experiments were approved by the institutional animal care and experiment committee at Hokkaido University. We subcutaneously injected 1×10^6 B16/F10 murine melanoma cells into the mice, measured the tumor size by surface examination every 4 d, and excised the tumors 16 d post-implantation for further analyses. Tumor volume was calculated by long and short axes and height, where each tumor was assumed to be an ellipsoid (19). CD31-positive infiltrating microvessels were counted in 10 fields per section from 4 mice per group. Abdominal and thoracic organs were also dissected to determine whether there were any

metastases. We deem noteworthy that the cell line used here is reported to metastasize to the lungs by intravenous injection, but not by subcutaneous injection (20).

The Aortic ring assay was performed essentially as described previously (21). Briefly, thoracic aortae obtained from WT and KO mice were sectioned, placed on a well of a 48-well plate coated with 125 μl of Matrigel, and covered with an additional 100 μl of Matrigel. The rings were incubated in 500 μl of complete EGM-2. The medium was replaced every other day. At day 5, images of aortic rings were acquired, and the outgrowth areas were delineated and quantitated with MetaMorph software (Molecular Devices, West Chester, PA).

Invasion, migration, and wound-healing assays. The Matrigel invasion assay was performed using 24-well BD BioCoat Matrigel Invasion Chambers (BD-Discovery). HUVECs (2.5×10^4) were seeded in the upper chamber in serum- and supplement-free EGM-2 medium. Cells were allowed to invade to the lower chamber containing complete EGM-2 medium for 22 h. The non-invading cells on the upper surface of the filter were removed by wiping with a cotton swab. Infiltrated cells were fixed with 3.7% formaldehyde in PBS, stained with 0.2% crystal violet, and quantified. For the migration assay to type I collagen gels, a transwell (Nunc AS, Roskilde, Denmark) was coated with a type I-P collagen solution (Nitta Gelatin, Osaka, Japan) for 1 h at 37°C, and washed twice with EGM-2 medium. After inoculation with 1.0×10^4 cells and incubation for 8 h, analysis was performed as described above. The wound-healing assay was performed as described previously (18).

Chromatin immunoprecipitation assay. A Chromatin Immunoprecipitation (ChIP) Assay Kit (upstate, Lake Placid, NY) was used essentially according to the manufacturer's protocol. Briefly, control and HA-TCF8-expressing 293T cells were fixed with 1% formaldehyde, lysed in lysis buffer, sonicated, and clarified by centrifugation. The resulting supernatant was immunoprecipitated with an anti-HA antibody. The precipitates were then amplified by PCR with these primers: Mmp1-promoter-F, 5'-

AGCCACCGTAAAGTGAGTGC-3’; Mmp1-promoter-R, 5’-TTTCTCCACACACCTTGCTC-3’; and Mmp1-3'-CDR-F, 5’-TGCAACTCTGACGTTGATCC-3’; Mmp1-3'-CDR-R, 5’-GGTGACACCAGTGACTGCAC-3’.

Cell adhesion and permeability assay. The cell adhesion assay was performed essentially as described previously (22). After coating wells with Matrigel or type I-C collagen (Nitta Gelatin) for 1 h at room temperature, 2×10^4 HUVECs were plated in each well of a 96-well plate (Nunc) for the indicated time at 37°C. The bound cells were stained with 0.04% crystal violet, lysed, and quantified by measuring the absorbance at 595 nm.

Cell permeability was determined by using an In Vitro Vascular Permeability Assay kit (CHEMICON International, Temecula, CA) according to the manufacturer’s instructions.

Immunohistochemistry and fluorescence microscopy. Formalin-fixed paraffin sections were stained with hematoxylin and eosin (HE) by the conventional method. The sections were also incubated in primary antibodies, peroxidase blocking solution, biotinylated secondary antibody, avidin/biotin C solution, and peroxidase substrate solution. Microscopic examination was performed after counterstaining with hematoxylin. Immunofluorescence microscopy was performed as described (23).

Statistical analyses. All data represent means and standard deviations of three independent experiments performed in triplicate, and were subjected to one-way analysis of variance, followed by the comparison by Student's or Welch's t-tests. P values obtained from the tests are described in the figure legends.

Results

TCF8 expression during angiogenesis. To test whether TCF8 is involved in angiogenesis, we first examined the expression of TCF8 mRNA during tube formation of human umbilical vein endothelial cells (HUVECs) on Matrigel, an *in vitro* approximation of angiogenesis, and found that TCF8 expression was up-regulated ~2.5-fold at 12 h after initiation of tube formation by HUVECs on Matrigel (Fig. 1*A* and *B*). We also explored the mechanism by which the expression of TCF8 is regulated in HUVECs; however, none of the growth factors included in the assay medium could induce TCF8 expression (Fig. 1*C*), even in the combination of all factors (Supplementary Fig. S1). In particular, TGF-β, a known inducer of TCF8 especially in carcinomas (24), failed to evoke TCF8 expression in HUVECs (Fig. 1*C*), indicating a cell type-specific regulation.

To verify endothelial TCF8 expression *in vivo*, we performed immunohistochemistry on human pathological specimens using an anti-TCF8 antibody. The expression of TCF8 in human breast cancer tissue was observed in the hyalinized vascular structure (Fig. 1*D*, *a*—*c*), and TCF8-positive cells (Fig. 1*D*, *b* and *c*, arrow) were distinct from α-smooth muscle actin (SMA) positive cells (arrow head). Endothelial staining was more apparent in colon cancer vessels (Fig. 1*D*, *d*—*f*), and TCF8 expression was also detected in the sinusoidal endothelium of hepatocellular carcinoma, vasculatures of hemangioblastoma, and cavernous hemangioma (Supplementary Fig. S2*A*—*C*). In contrast, TCF8 was absent from granulation tissue capillaries, dilated malformed vessel endothelium, and normal blood vessels within intervening brain tissues (Fig. 1*D*, *g*—*i* and Supplementary Fig. S2*D*). These results indicate that TCF8 is preferentially expressed in the endothelial cells of tumor vessels, a location where vigorous angiogenesis occurs. When comparing the time courses of TCF8 induction and tube formation, we noticed that the tube architecture was nearly complete and at steady-state, at the time points of TCF8 induction (Fig. 1*A*—*C*), suggesting a role for TCF8 in the termination and stabilization, but not the induction, of tube formation. Therefore, TCF8 signaling might be needed to subdue excess tumor angiogenesis.

TCF8 regulates tumor angiogenesis *in vivo*. We next appraised the function of TCF8 in tumor angiogenesis *in vivo*. B16/F10 murine melanoma cells were injected subcutaneously into C57BL/6 mice and *δEf1*/*Tcf8*-heterozygous KO mice with a C57BL/6 background. As revealed by surface examination, implanted tumor growth in *Tcf8*-deficient mice was significantly slower during the first 12 d, but was comparable to WT mice at day 16 (Supplementary Fig. S3*A*). Macroscopic examination during autopsy revealed that the tumors had a complex, multi-lobular appearance and had invaded into adjacent and deeper tissues in *Tcf8*-mutant mice, whereas tumors in WT mice were encapsulated with simple oval shapes (Fig. 2*A* and *B*, and Supplementary Fig. S3*B*). This appeared to be the reason for the observed comparable tumor sizes between the mice. Consistent with its more aggressive features, the tumor weight of the mutant mice was significantly greater than that of the WT mice (Fig. 2*A*). Surprisingly, multiple lung metastases of up to 2 mm in diameter were observed in 3 out of the 4 mutant mice, but were not observed in WT animals (Fig. 2*C*). It is important to note that the F10 subline of B16 melanoma has never been shown to metastasize to distant organs following subcutaneous injection (20), indicating that the TCF8-deficient milieu allowed for the tumors to display more malignant phenotypes. Immunohistochemistry demonstrated that the number of microvessels composed of CD31-positive endothelial cells in KO mice tumors was significantly higher than that of WT mice (Fig. 2*D*), and that the expression of TCF8 in the endothelium of tumor vessels in these tumors was substantially less than that of their WT counterparts, notwithstanding the heterozygous nature of the KO mice, as opposed to a homozygous one (Fig. 2*D*). Although it is possible that the tumors are also influenced by signals emanating from other tumor stroma components, excess angiogenesis constitutes one of the foremost mechanisms in providing a favorable milieu for more aggressive tumor growth, thus highlighting the importance of these findings.

TCF8 negatively regulates angiogenesis *in vitro* and *ex vivo*. To further investigate the exact mechanism by which TCF8 regulates angiogenesis, we examined the effect of TCF8

expression on tube formation by HUVECs. Endogenous TCF8 knockdown by small interference RNAs (siRNAs), which successfully suppress expression by 70-80% (Fig. 3*A*), augmented the number of tubes ~2-fold in Matrigel (Fig. 3*B*). Essentially similar results were obtained by tube formation on a type I collagen gel (data not shown). Furthermore, when we performed an aortic ring assay (an *ex vivo* angiogenic model) by utilizing sections of aortae resected from *Tcf8*-heterozygous KO and wild-type mice, endothelial cell sprouting from the aortae of KO mice was again more efficient than those of wild-type (WT) mice (Fig. 3*C*). One should also note that the knockdown of TCF8 enhances tube formation but the tube structure is easily breakable and unstable. These results clearly indicate a critical role for TCF8 in the negative regulation as well as stabilization of angiogenesis.

TCF8 regulates cell invasion and migration via MMP1 expression. We next examined the effect of TCF8 expression on the cellular phenotypes involved in angiogenic processes, including cell invasiveness, motility, and adhesion (4, 25). Consistent with the results of the tube formation assay, invasiveness into Matrigel was enhanced up to 2.3-fold by transfection with siRNAs against TCF8 (Fig. 4*A*). Enhanced migration, ~3.7-fold, when a type I collagen gel was used as a matrix, was also observed (Fig. 4*A*). Interestingly, however, TCF8 is likely to be dispensable for endothelial cell motility. A wound-healing assay demonstrated no significant differences in the motility of HUVECs transfected with control and TCF8-targeting siRNA on the matrices tested (data not shown), unlike breast cancer cells in which TCF8 accelerates the motility (26).

One possible mechanism underlying the increased invasiveness and migration might be the up-regulated digestion of ECMs via TCF8-mediated transcriptional regulation of the gene encoding MMP1. *MMP1* induction during tube formation was significantly enhanced in Matrigel when TCF8 was silenced (Fig. 4*B*). Furthermore, a chromatin immunoprecipitation assay demonstrated the specific binding of TCF8 to the promoter region of the *Mmp1* gene (Fig. 4*C*), in which there are two putative TCF8 binding sites at -427 and -409 bp from the transcription

initiation site (data not shown). To verify the significance of MMP1 as a downstream effector of TCF8, we performed a tube formation assay in the presence or absence of an MMP inhibitor, GM6001, and found that tube formation, facilitated by TCF8 knockdown, was inhibited by GM6001 by approximately 20% (Fig. 4*D*), suggesting that, albeit in part, MMP1 plays a substantial role in TCF8-mediated regulation of angiogenesis. These data collectively indicate that TCF8, induced in the late phase of angiogenesis, regulates MMP1 expression negatively, thereby blocking invading endothelial cells.

TCF8 regulates cell-matrix and cell-cell adhesions. The other cellular function of TCF8 involves cell adhesion. TCF8 silencing significantly inhibited cell adhesion to both Matrigel and type I collagen by > 25%, whereas the plating efficiency toward uncoated culture plates was not altered (Fig. 5*A*). Focal adhesions of TCF8-silenced cells were increased in number but decreased in size, with fine actin filaments visualized by anti-paxillin and phalloidin (Fig. 5*B*), suggesting that TCF8 is required for the consolidation of integrin-mediated interactions to the specific ECMs.

TCF8 may also participate in the regulation of cell-cell adhesion. We found that TCF8-repressed HUVECs allowed for more 70,000-molecular weight dextran penetration through the cell monolayer than control siRNA-treated HUVECs (Fig. 5*C*). By visualizing cell-cell adhesion with an antibody against the key molecule of endothelial adherence junction, VE-cadherin, cell-cell contacts without the VE-cadherin recruitment were specifically observed in the TCF8-suppressed cells (Fig. 5*D*, arrow heads); whereas the staining pattern of the tight junction component molecule ZO-1 was comparable (data not shown), which is in agreement with a very recent report (27). It is interesting that TCF8 repression did not affect the expression level of *VE-cadherin* (data not shown). Therefore, it seems that TCF8 specifically regulates the recruitment of VE-cadherin to the membrane, possibly by altering the expression level of regulators of VE-cadherin localization; however, further in-depth studies are required. In view of these results, it

appears that TCF8 plays a key role in the strengthening of cell-matrix and cell-cell adhesion, which in turn might be substantially important in the stabilization of vasculature.

Discussion

In the present study, we show that TCF8, expressed specifically in endothelial cells and induced in the late phase of *in vitro* angiogenesis models, plays an integral role in the regulation of angiogenesis by regulating cell invasiveness, adhesiveness, and permeability. These observations, consistent with the phenotype seen in *Tcf8*$^{-/-}$ embryos having frequent edema at midgestation and, less frequently, internal bleeding in the nasal region (10), indicate that vasculatures comprised of TCF8-repressed endothelial cells are unsettled and leaky, albeit devoid of the structural abnormalities of the vasculature in the mutant mice (10). These characteristics of TCF8-deficient vessels resemble those of tumor vessels, which lead to increased interstitial pressure that limits drug diffusion within the tumor and favors tumor spreading, which occasionally leads to tumor cell dissemination in the blood stream and the appearance of tumor metastases (28). TCF8 expressed in tumor vessels is probably required for the suppression of excess tumor angiogenesis. Indeed, allograft tumors in *Tcf8*-deficient mice display aggressive growth and lung metastases (Fig. 2).

Cancer development and progression are attributed to genetic and epigenetic alterations in transforming cells. However, tumors are not merely a unitary aggregate of neoplastic cells, but rather a complex tissue with ECMs, blood vessels, stromal cells, and infiltrating immune cells. Tumor angiogenesis is the most critical biological event for cancer progression, not only because it supplies oxygen for tumor growth, but also because it supports tumor invasion, metastases, and drug resistance (28). VEGF inhibitors, such as bevacizumab—an anti-VEGF antibody approved by the US Food and Drug Administration for use in colorectal and breast cancers—have been shown to reduce tumor volumes and increase progression-free survival time; however, monotherapy is insufficient for the complete suppression of tumor angiogenesis. Rather, there are concerns about upregulation of other classes of angiogenic factors and the emergence of side effects (7). Notwithstanding that further detailed studies are required to identify the cell type in which TCF8 functions as a negative regulator of tumor angiogenesis, our observations provide

clear evidence that TCF8 in the tumor microenvironment plays a crucial role in this process, and hence may offer a VEGF-independent target for use in the therapeutics of tumor angiogenesis suppression.

It has been reported that several humoral factors, including BMP-6, TGF-β, HB-EGF, and estrogen, possess the ability to regulate TCF8 expression (29-32). Although we tested the involvement of stimulants in TCF8 regulation, TGF-β, even in combination with other stimulants, unexpectedly fails to induce TCF8 expression in the endothelial cell context (Fig. 1*C* and Supplementary Fig. S1). Therefore, we hypothesize that the expression of TCF8 might be regulated in a manner particular to endothelial cells, and hence the exploration of factor(s) that act specifically on endothelial cells to induce TCF8 expression will be fundamental to establish TCF8-targeted therapy. In this regard, angiotensin II (AII) signaling might be a possible candidate. Firstly, AII, which binds to two distinct cell surface receptors, angiotensin type 1 and type 2 receptors (AT1R and AT2R), is implicated in tumor angiogenesis [reviewed in (33-36)], and it is also reported that the engagement of AII to AT2R induces TCF8 expression (37). Moreover, our very preliminary data indicate that HUVECs express both AT1R and AT2R, and that TCF8 expression is induced by AII[4]. In view of the above, AII stimulation in the presence of AT1R inhibitors is anticipated as an ideal therapeutic intervention, through which TCF8 expression is specifically introduced in endothelial cells.

TCF8 has been extensively implicated in the epithelial-mesenchymal transition (EMT) of cancer cells, characterized by loss of the epithelial phenotype and the acquisition of a mesenchymal state, where it acts as a transcriptional repressor for a wide range of genes encoding epithelial marker proteins, including E-cadherin and Lgl2, by binding directly to their promoter regions (8, 26, 38). Since MMP1 expression was highly up-regulated in endothelial cells deficient in TCF8 (Fig. 4*B*), we can say that the function of TCF8 as a transcriptional attenuator is conserved in the endothelial cell lineage. However, even though its molecular

function is conserved, TCF8 develops different phenotypes in cancerous and endothelial cells; promoting EMT and inhibiting endothelial-mesenchymal transition (End-MT), respectively.

End-MT has been shown to play a key role in vascular remodeling and tumor angiogenesis (39-41), and, analogously to EMT, is characterized by loss of endothelial markers and an increase in mesenchymal markers, impaired cell-cell contact and adhesion, as well as an enhanced cell migration and secretion of proteases. Therefore, since the expression of TCF8 is induced in the late phase of angiogenesis and is dispensable for gene regulation of endothelial and mesenchymal markers, we propose that TCF8 is more likely to be a promoter of mesenchymal-endothelial re-transition, rather than an inhibitor of End-MT, as confirmed by the inhibition of MMP1 expression, consolidation of focal adhesion formation, and the recruitment of VE-cadherin, all of which play a critical role in keeping tumor vasculature remodeling in check.

Acknowledgements

We thank K. Kawakami for providing us with an antibody against TCF8 (AREB6), K. Hida and J. Hamada for providing cells, K. Shimizu, E. Aoyanagi, and N. Toyoda for technical assistance, S. Darmanin for critical reading of the manuscript, and J. Yamashita and the members of our laboratory for helpful discussions.

References

1. Folkman J. Angiogenesis: an organizing principle for drug discovery? Nat Rev Drug Discov 2007; 6: 273-86.
2. Carmeliet P. Angiogenesis in life, disease and medicine. Nature 2005; 438: 932-6.
3. Risau W. Mechanisms of angiogenesis. Nature 1997; 386: 671-4.
4. Adams RH, Alitalo K. Molecular regulation of angiogenesis and lymphangiogenesis. Nat Rev Mol Cell Biol 2007; 8: 464-78.
5. Impagnatiello MA, Weitzer S, Gannon G, Compagni A, Cotten M, Christofori G. Mammalian sprouty-1 and -2 are membrane-anchored phosphoprotein inhibitors of growth factor signaling in endothelial cells. J Cell Biol 2001; 152: 1087-98.
6. Hicklin DJ, Ellis LM. Role of the vascular endothelial growth factor pathway in tumor growth and angiogenesis. J Clin Oncol 2005; 23: 1011-27.
7. Casanovas O, Hicklin DJ, Bergers G, Hanahan D. Drug resistance by evasion of antiangiogenic targeting of VEGF signaling in late-stage pancreatic islet tumors. Cancer Cell 2005; 8: 299-309.
8. Peinado H, Olmeda D, Cano A. Snail, Zeb and bHLH factors in tumour progression: an alliance against the epithelial phenotype? Nat Rev Cancer 2007; 7: 415-28.
9. Zwijsen A, van Grunsven LA, Bosman EA, et al. Transforming growth factor beta signalling in vitro and in vivo: activin ligand-receptor interaction, Smad5 in vasculogenesis, and repression of target genes by the deltaEF1/ZEB-related SIP1 in the vertebrate embryo. Mol Cell Endocrinol 2001; 180: 13-24.
10. Takagi T, Moribe H, Kondoh H, Higashi Y. DeltaEF1, a zinc finger and homeodomain transcription factor, is required for skeleton patterning in multiple lineages. Development 1998; 125: 21-31.

11. Higashi Y, Moribe H, Takagi T, et al. Impairment of T cell development in deltaEF1 mutant mice. J Exp Med 1997; 185: 1467-79.

12. Nishimura G, Manabe I, Tsushima K, et al. DeltaEF1 mediates TGF-beta signaling in vascular smooth muscle cell differentiation. Dev Cell 2006; 11: 93-104.

13. Krafchak CM, Pawar H, Moroi SE, et al. Mutations in TCF8 cause posterior polymorphous corneal dystrophy and ectopic expression of COL4A3 by corneal endothelial cells. Am J Hum Genet 2005; 77: 694-708.

14. Terai K, Matsuda M. Ras binding opens c-Raf to expose the docking site for mitogen-activated protein kinase kinase. EMBO Rep 2005; 6: 251-5.

15. Eger A, Aigner K, Sonderegger S, et al. DeltaEF1 is a transcriptional repressor of E-cadherin and regulates epithelial plasticity in breast cancer cells. Oncogene 2005; 24: 2375-85.

16. Davis GE, Senger DR. Endothelial extracellular matrix: biosynthesis, remodeling, and functions during vascular morphogenesis and neovessel stabilization. Circ Res 2005; 97: 1093-107.

17. Potente M, Urbich C, Sasaki K, et al. Involvement of Foxo transcription factors in angiogenesis and postnatal neovascularization. J Clin Invest 2005; 115: 2382-92.

18. Yamada T, Tsuda M, Ohba Y, Kawaguchi H, Totsuka Y, Shindoh M. PTHrP promotes malignancy of human oral cancer cell downstream of the EGFR signaling. Biochem Biophys Res Commun 2008; 368: 575-81.

19. Whitmore MM, Li S, Falo L, Jr., Huang L. Systemic administration of LPD prepared with CpG oligonucleotides inhibits the growth of established pulmonary metastases by stimulating innate and acquired antitumor immune responses. Cancer Immunol Immunother 2001; 50: 503-14.

20. Passaniti A, Hart GW. Cell surface sialylation and tumor metastasis. Metastatic potential of B16 melanoma variants correlates with their relative numbers of specific penultimate oligosaccharide structures. J Biol Chem 1988; 263: 7591-603.

21. Min JK, Cho YL, Choi JH, et al. Receptor activator of nuclear factor (NF)-kappaB ligand (RANKL) increases vascular permeability: impaired permeability and angiogenesis in eNOS-deficient mice. Blood 2007; 109: 1495-502.

22. Linghu H, Tsuda M, Makino Y, et al. Involvement of adaptor protein Crk in malignant feature of human ovarian cancer cell line MCAS. Oncogene 2006; 25: 3547-56.

23. Ohba Y, Mochizuki N, Yamashita S, et al. Regulatory proteins of R-Ras, TC21/R-Ras2, and M-Ras/R-Ras3. J Biol Chem 2000; 275: 20020-6.

24. Shirakihara T, Saitoh M, Miyazono K. Differential regulation of epithelial and mesenchymal markers by deltaEF1 proteins in epithelial mesenchymal transition induced by TGF-beta. Mol Biol Cell 2007; 18: 3533-44.

25. Veeravagu A, Hsu AR, Cai W, Hou LC, Tse VC, Chen X. Vascular endothelial growth factor and vascular endothelial growth factor receptor inhibitors as anti-angiogenic agents in cancer therapy. Recent Patents Anticancer Drug Discov 2007; 2: 59-71.

26. Spaderna S, Schmalhofer O, Wahlbuhl M, et al. The transcriptional repressor ZEB1 promotes metastasis and loss of cell polarity in cancer. Cancer Res 2008; 68: 537-44.

27. Taddei A, Giampietro C, Conti A, et al. Endothelial adherens junctions control tight junctions by VE-cadherin-mediated upregulation of claudin-5. Nat Cell Biol 2008; 10: 923-34.

28. Neri D, Bicknell R. Tumour vascular targeting. Nat Rev Cancer 2005; 5: 436-46.

29. Comijn J, Berx G, Vermassen P, et al. The two-handed E box binding zinc finger protein SIP1 downregulates E-cadherin and induces invasion. Mol Cell 2001; 7: 1267-78.

30. Postigo AA. Opposing functions of ZEB proteins in the regulation of the TGFbeta/BMP signaling pathway. EMBO J 2003; 22: 2443-52.

31. Postigo AA, Depp JL, Taylor JJ, Kroll KL. Regulation of Smad signaling through a differential recruitment of coactivators and corepressors by ZEB proteins. EMBO J 2003; 22: 2453-62.

32. Wang F, Sloss C, Zhang X, Lee SW, Cusack JC. Membrane-bound heparin-binding epidermal growth factor like growth factor regulates E-cadherin expression in pancreatic carcinoma cells. Cancer Res 2007; 67: 8486-93.

33. Deshayes F, Nahmias C. Angiotensin receptors: a new role in cancer? Trends Endocrinol Metab 2005; 16: 293-9.

34. Escobar E, Rodriguez-Reyna TS, Arrieta O, Sotelo J. Angiotensin II, cell proliferation and angiogenesis regulator: biologic and therapeutic implications in cancer. Curr Vasc Pharmacol 2004; 2: 385-99.

35. Molteni A, Heffelfinger S, Moulder JE, Uhal B, Castellani WJ. Potential deployment of angiotensin I converting enzyme inhibitors and of angiotensin II type 1 and type 2 receptor blockers in cancer chemotherapy. Anticancer Agents Med Chem 2006; 6: 451-60.

36. Yoshiji H, Kuriyama S, Noguchi R, Fukui H. Angiotensin-I converting enzyme inhibitors as potential anti-angiogenic agents for cancer therapy. Curr Cancer Drug Targets 2004; 4: 555-67.

37. Stoll M, Hahn AW, Jonas U, et al. Identification of a zinc finger homoeodomain enhancer protein after AT(2) receptor stimulation by differential mRNA display. Arterioscler Thromb Vasc Biol 2002; 22: 231-7.

38. Remacle JE, Kraft H, Lerchner W, et al. New mode of DNA binding of multi-zinc finger transcription factors: deltaEF1 family members bind with two hands to two target sites. EMBO J 1999; 18: 5073-84.

39. Andrae J, Gallini R, Betsholtz C. Role of platelet-derived growth factors in physiology and medicine. Genes Dev 2008; 22: 1276-312.

40. Arciniegas E, Frid MG, Douglas IS, Stenmark KR. Perspectives on endothelial-to-mesenchymal transition: potential contribution to vascular remodeling in chronic pulmonary hypertension. Am J Physiol Lung Cell Mol Physiol 2007; 293: L1-8.

41. Ghersi G. Roles of molecules involved in epithelial/mesenchymal transition during angiogenesis. Front Biosci 2008; 13: 2335-55.

Figure Legends

Figure 1. TCF8 expression during angiogenesis. ***A*** and ***B,*** HUVECs were seeded on Matrigel and subjected to an *in vitro* tube formation assay. Expression levels of *TCF8* at the indicated time points were determined by conventional (left panels) and real-time (right) RT-PCR. Representative photographs are also shown (*B*). ***C,*** HUVECs were serum-starved for 16 h, and then stimulated by growth factors (denoted at the top) for the indicated times. The expression levels of *TCF8* and *GAPDH* were determined as in (A). ***D,*** Expression of TCF8 in tumor vessels. Formalin-fixed paraffin-embedded specimens of the tissues described at the top were subjected to hematoxylin and eosin staining (HE) and immunohistochemistry with anti-TCF8 and α-SMA. An arrow and arrow head indicate cells expressing TCF8 and α-SMA, respectively (*b*, *c*). ***f*** and ***i,*** Magnifications of the insets in (e) and (h).

Figure 2. Haploinsufficiency of TCF8 leads to excess angiogenesis and aggressive growth of implanted melanoma. WT or *Tcf8*/*δEf1* heterozygous KO (KO) mice were subcutaneously injected with murine B16/F10 melanoma cells. At 16 d post-implantation, the mice were sacrificed and examined. ***A,*** Macroscopic photographs of excised tumors from WT and KO mice (left). The tumors were weighed and the mean weight of four tumors is shown with standard deviations for both groups (right). *, $P = 0.0159$. ***B,*** Excised tumor tissues were fixed with 10% formalin, embedded in paraffin, and stained with HE. Microscopic photographs of tumors formed in WT and KO mice are shown. The right panel is a magnification of the inset, revealing tumor invasion into striated muscle. ***C,*** Macroscopic and microscopic photographs of the lungs. Metastatic nodules are indicated by arrow heads (left). The right hand side photograph is a magnification of the inset, indicating metastatic nodules and tumor thrombi (right). ***D,*** Microscopic photographs of tumors stained with HE, and antibodies against CD31 and TCF8. The number of blood vessels visualized by CD31 staining was quantified by calculating the means of 10 fields per section from 4 mice per group. They are shown in the graph with standard deviations. *, $P = 0.000586$. HPF, high-power field.

Figure 3. Negative regulation of angiogenesis by TCF8. ***A,*** HUVECs were transfected with TCF8-targeting siRNA (si TCF8) or a scramble siRNA (si Control). After 48 h, TCF8 mRNA levels (upper panels) and protein levels (lower panels) were determined. ***B,*** HUVECs prepared as in (*A*) were subjected to a tube formation assay and photographed (lower photographs). The tube number was counted and plotted at the indicated time. The means of triplicates from three independent experiments are shown with standard deviations. *, $P = 0.00956$; **, $P = 0.00532$. ***C,*** Aortic rings dissected from WT or *Tcf8*/*δEF1*-heterozygous KO (KO) mice were embedded in Matrigel. After 5 d, the areas of endothelial sprouting were quantified. The means of triplicates are plotted with standard deviations. *, $P = 0.00621$. Representative photographs are shown.

Figure 4. TCF8 regulates cell invasiveness and migration via MMP1 expression. ***A,*** HUVECs transfected with si Control or si TCF8 were inoculated on Matrigel-coated or on type I collagen (Col-I)-coated chambers. After 22 h (Matrigel) or 8 h (Col-I), the invading/migrating cells were counted, and means of triplicates from three independent experiments plotted with standard deviations. *, $P = 0.00514$; **, $P = 0.00127$. Representative photographs are shown. ***B,*** Levels of *MMP1* during tube formation were determined by real-time RT-PCR. The data shown are means of triplicates from three independent experiments. ***C,*** Chromatin immunoprecipitation assay to confirm TCF8-*Mmp1* promoter interaction. Immunoprecipitates (upper panel) of lysates of 293T cells expressing HA-TCF8 or input DNA (lower panel) were amplified by primers specific for the human *Mmp1* promoter (promoter) or 3'-coding (CDR) regions. ***D,*** HUVECs prepared as in (*A*) were subjected to a tube formation assay in the presence or absence of an MMP inhibitor GM6001. The data shown are means of triplicates from three independent experiments. *, $P = 0.00939$; **, $P = 0.00186$; ***, $P = 0.0152$.

Figure 5. TCF8 regulates cell-matrix and cell-cell adhesion. ***A,*** HUVECs transfected with si Control or si TCF8 were plated onto Matrigel-coated, type I collagen–coated, or uncoated 96-well plates for 15 min. The bound cells were stained with crystal violet and quantified. The data shown are means of triplicates from three independent experiments. *, $P = 0.00706$; **, $P =$

0.000130. ***B*** and ***D,*** Cells prepared as in (A) were fixed with 3% paraformaldehyde, permeabilized, and incubated with anti-paxillin (*B*) and anti-VE-cadherin (*D*) antibodies, followed by further incubation with Alexa-488–conjugated anti-mouse secondary antibody. F-actin was visualized by phalloidin, and the right hand panels represent merged photographs. Second column panels in the upper row are magnifications of the left insets. ***C,*** Cell permeability assay for HUVECs transfected with si Control or si TCF8 (right). The fluorescence intensity of the lower chamber medium was measured and the means of triplicates from three independent experiments were plotted. ***, $P = 0.0241$

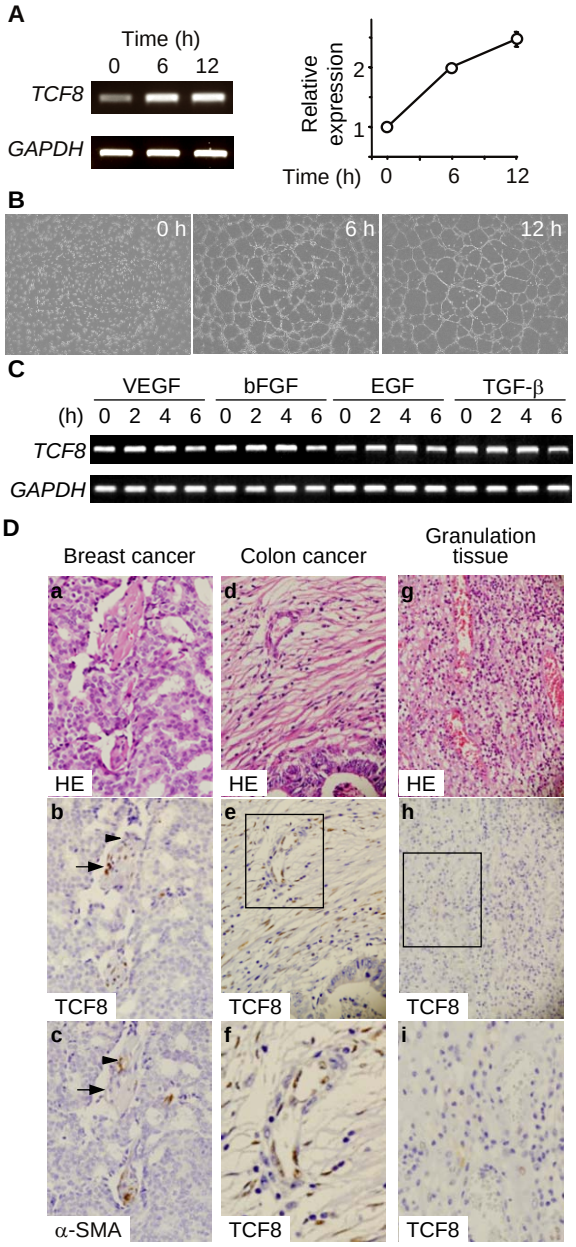

Figure 1. Inuzuka, T., *et al.*

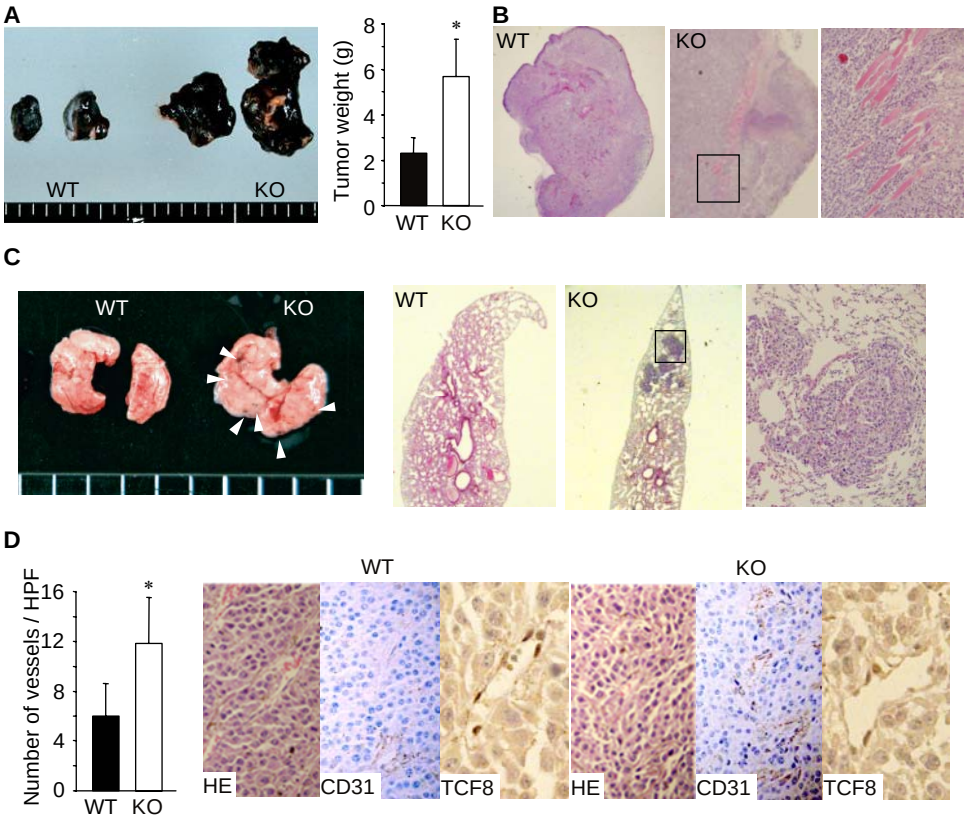

Figure 2. Inuzuka, T., *et al.*

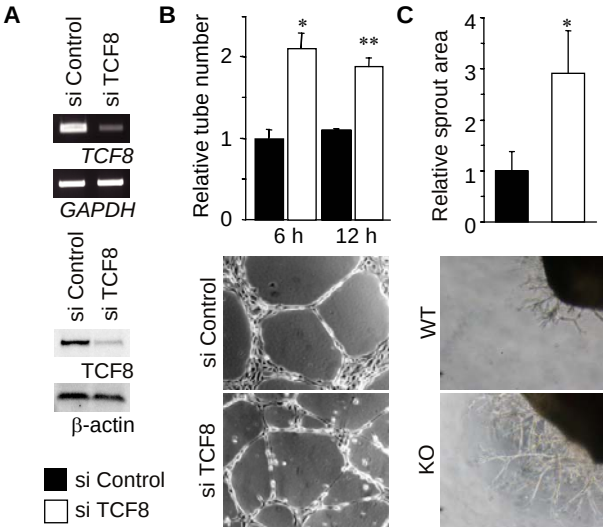

Figure 3. Inuzuka, T., *et al.*

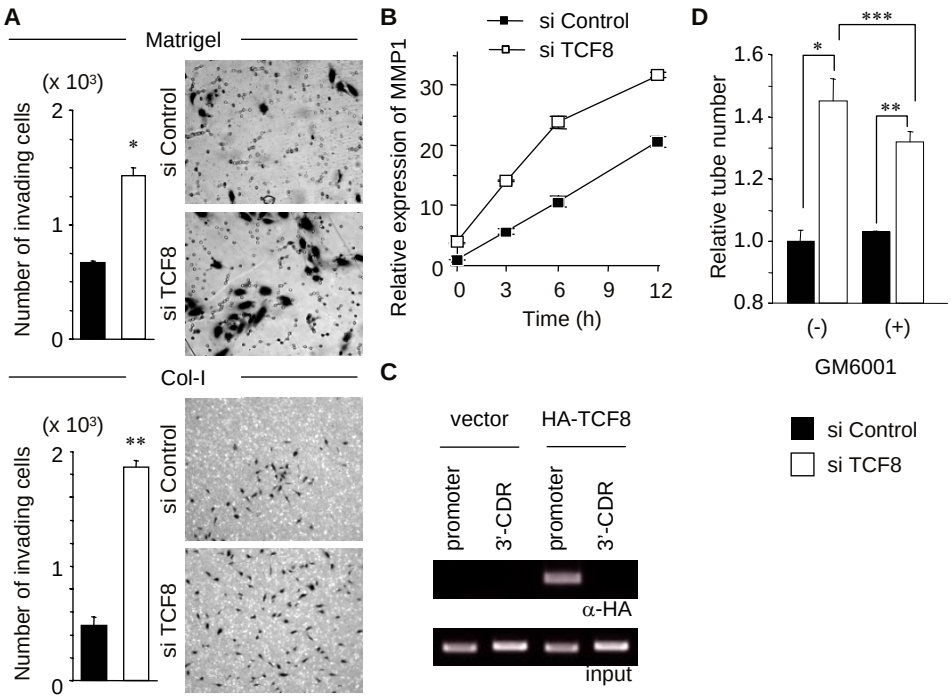

Figure 4. Inuzuka, T., *et al.*

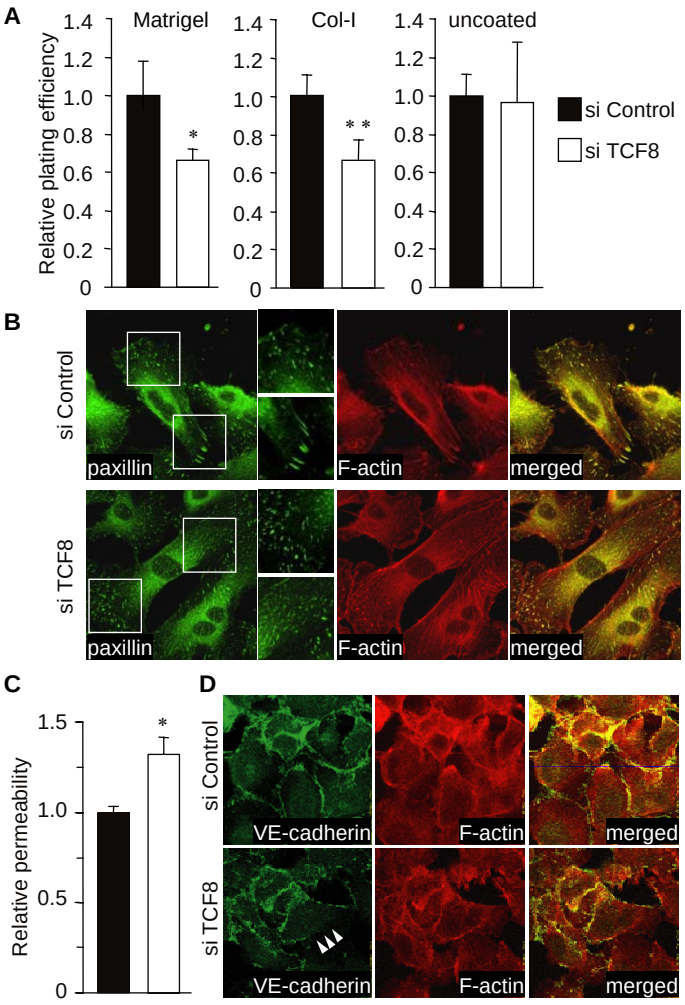

Figure 5. Inuzuka, T., *et al.*

Supplementary Figure S1. Inuzuka, T., *et al.*

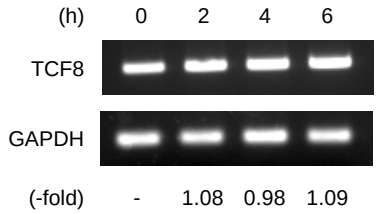

Supplementary Figure S1. Growth factors failed to induce TCF8 expression. HUVECs were serum-starved for 16 h, and then stimulated by the combination of VEGF, bFGF, EGF, and TGF-β for the times indicated. The expression levels of *TCF8* and *GAPDH* were determined as in Figure 1*C*.

Supplementary Figure S2. Inuzuka, T., *et al.*

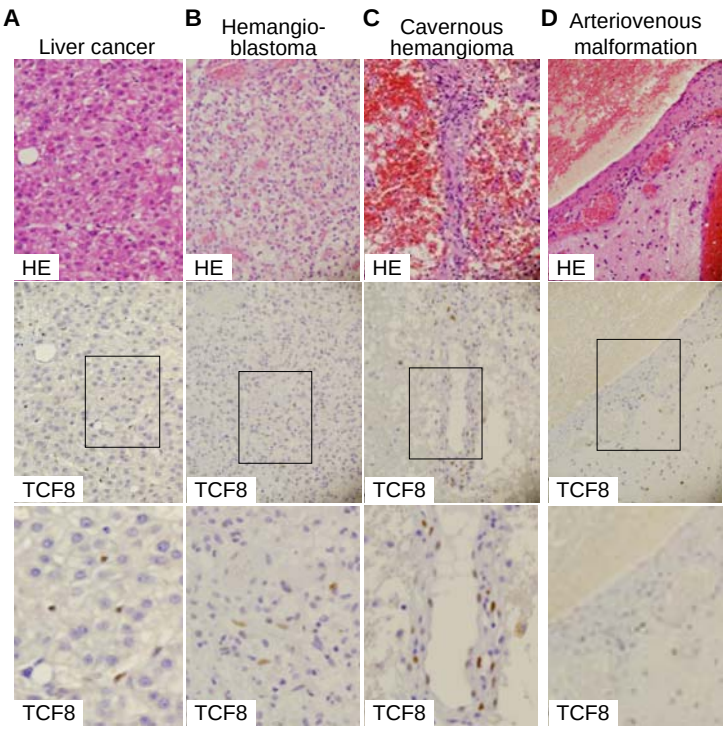

Supplementary Figure S2. Expression of TCF8 in tumor vessels. Photographs of HE staining and immunostaining with anti-TCF8 of indicated tissues are shown. The bottom panels are magnifications of the middle insets.

Supplementary Figure S3. Inuzuka, T., *et al.*

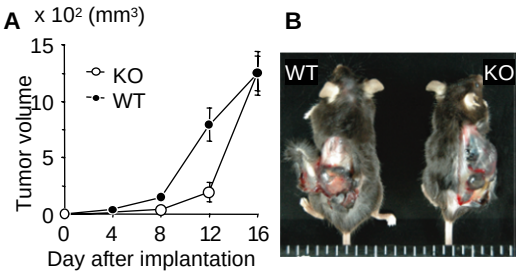

Supplementary Figure S3. Aggressive growth of implanted melanoma in *Tcf8*$^{+/-}$ KO mice. WT or *Tcf8*/*δEf1* heterozygous KO (KO) mice were subcutaneously injected with B16/F10 cells. ***A,*** Long and short axes and height were measured from the body surface every 4 d and tumor volumes were calculated assuming an ellipsoid shape. ***B,*** Tumors after skin incision.